Reduced Models of Magnetohydrodynamic Turbulence in the Interstellar Medium and the Solar Wind

A. Bhattacharjee and C. S. Ng

Department of Physics and Astronomy, The University of Iowa,
Iowa City, Iowa 52242, USA

Abstract. Recent developments in the derivation of reduced models for weakly compressible magnetohydrodynamic (MHD) turbulence are discussed. A four-field system of equations has been derived from the compressible magnetohydrodynamic (MHD) equations to describe turbulence in the interstellar medium and the solar wind. These equations apply to a plasma permeated by a spatially varying mean magnetic field when the plasma beta is of the order unity or less. In the presence of spatial inhomogeneities, the four-field equations predict pressure fluctuations of the order of the Mach number of the turbulence, as observed by Helios 1 and 2. In the presence of a uniform background field and a spatially homogeneous plasma, the four-field system reduces to the so-called nearly incompressible system. In the weak-turbulence limit, dominated by three-wave interactions, the anisotropic energy spectrum is deduced by a combination of exact analytical results and numerical simulations.

1 Introduction

Magnetohydrodynamics (MHD), despite its significant limitations as a model, provides the principal framework for the theoretical description of turbulence in the interstellar medium (ISM) and the solar wind. There is strong observational evidence that the effect of plasma compressibility cannot be neglected in theoretical studies of magnetohydrodynamic (MHD) turbulence in these systems. This should not be all that surprising, for the plasma beta in the solar wind and the ISM is often of the order unity or greater. Consequently, the sound speed is of the same order of magnitude or greater than the Alfvén speed. (In a truly incompressible plasma, the sound speed is infinitely large.) Hence, the assumption of constant plasma density (ρ), which is sufficient to ensure that the plasma flow velocity $\boldsymbol{v}$ obeys the incompressibility condition $\nabla\cdot\boldsymbol{v} = 0$ by the continuity equation $\partial\rho/\partial t+\nabla\cdot(\rho\boldsymbol{v}) = 0$, cannot be sustained.

Since the observed fluctuations in the solar wind and the ISM involve density variations, it is widely appreciated that the effects of plasma compressibility should be incorporated in a viable theory of MHD turbulence for such systems. However, theoretical attempts to grapple with compressible turbulence from first principles are hampered by the formidable analytical (as well as numerical) complexities of the fully compressible MHD equations which involve eight scalar variables (i.e., three components each for the fluid velocity and magnetic fields, the plasma density, and pressure) and several nonlinearities. Even in simple magnetic geometry, it is difficult to obtain numerically a reliable inertial range spectrum (spanning a few decades in wavenumber) for compressible MHD turbulence.

In view of these difficulties, attempts have been made (primarily in the theoretical solar wind literature) to derive reduced MHD models that can enable the computation of compressible turbulence as perturbative corrections to a leading-order incompressible description. Perhaps the most well-known of such attempts is the nearly incompressible MHD (NI-MHD) model of Zank and Matthaeus [1,2] (hereafter, ZM). The NI-MHD model formulated by ZM has its antecedents in the pseudosound theory of Lighthill [3] for compressible hydrodynamic (HD) turbulence. Lighthill's work provided the stimulus for analogous MHD applications by Montgomery et al. [4], Shebalin and Montgomery [5], and Matthaeus and Brown [6] as well as the development of nearly incompressible HD [7] which preceded the development of NI-MHD by ZM. Independently, Grappin et al. [8] have pointed out that the MHD variant of pseudosound theory can also be viewed as an extension of the HD theory of Kliatskin [9].

In its basic form, the equations of the NI-MHD model are similar to those of the reduced MHD (RMHD) model [10] which has proved to be extremely useful in describing nonlinear MHD dynamics in tokamak or solar coronal plasmas. (The derivation of NI-MHD given by ZM suggests that RMHD is a subset of NI-MHD.) Tokamak as well as solar coronal plasmas are typically permeated by a strong magnetic field and characterized by low values of the plasma beta (β) (that is, $\beta \ll 1$). Exploiting the fact that solar wind turbulence in the plasma frame is characterized by low values of the turbulent Mach number, ZM show, by means of an asymptotic expansion in powers of the Mach number, that the equations of compressible MHD reduce to the NI-MHD equations.

One of the interesting but surprising conclusions of ZM is that the NI-MHD equations are valid for solar wind plasmas even when $\beta \sim 1$. Since the pressure fluctuations in the NI-MHD equations are decoupled, at leading order, from the dynamical equation for the velocity field fluctuations, ZM claim that compressible fluctuations are enslaved to incompressible dynamics. If true, this result is a remarkable simplification of the problem of compressible MHD turbulence in the solar wind (as well as in parts of the ISM) because one can then rely on analytical or numerical results derived from a leading-order incompressible MHD calculation and calculate the higher-order density fluctuations convected passively by an incompressible flow field.

The NI-MHD theory predicts that the root-mean-square pressure fluctuation (normalized by the background plasma pressure) in the solar wind should be $O(M^2)$, where M is the Mach number of the turbulence. This prediction has been tested by detailed comparison with observations from Voyager as well as Helios 1 and 2 [11–13]. From Fig. 3 of Tu and Marsch [12], who considered a large dataset from Helios 1 and 2 between 1 and 7 AU, we see that although there some data points are $O(M^2)$ scaling, most of the data points are distributed in the range between $O(M^2)$ and $O(M)$.

Motivated in part by these discrepancies between observations and the NI-MHD model, Bhattacharjee, Ng and Spangler [14] (hereafter, BNS) have formulated a new system of reduced equations for MHD turbulence, referred to hereafter as the four-field equations, valid for $\beta \sim 1$ plasmas. They too assume, following ZM, that the plasma is permeated by a background magnetic field and that the Mach number of the turbulence is small. However, unlike ZM who assume that the background magnetic field is spatially uniform, BNS allow the background field to be spatially nonuniform and capable of sustaining a nonvanishing plasma current density and pressure gradient. BNS then show that the compressible, three-dimensional (3D) MHD equations can be simplified to a system involving four scalar variables: the magnetic flux, the parallel vorticity (i.e., the component of vorticity parallel to the mean magnetic field), the perturbed pressure, and the parallel flow. This four-field system represents a generalization of NI-MHD (a two-field system at leading order) to plasmas with $\beta \leq 1$, and includes NI-MHD as a special case. The four-field system reduces to NI-MHD when (i) the background magnetic field is constant in space and all spatial inhomogeneities in the background quantities are neglected, and/or (ii) when $\beta \ll 1$. This reduction delineates clearly the restricted domain of applicability of NI-MHD, and suggests that although NI-MHD may apply to specific numerical experiments or to a selected subset of observations, it cannot be expected to account for as broad a dataset as shown in [12].

An important attribute of the four-field equations is that in a spatially inhomogeneous $\beta \sim 1$ plasma, the four field variables, that is, magnetic flux, parallel vorticity, pressure and parallel flow, are coupled to each other. This coupling has significant implications for the scaling of root-mean-square pressure fluctuations. In the presence of spatial inhomogeneities, the first-order pressure or density fluctuations evolve to non-zero values even if they are chosen to be zero initially, and modest inhomogeneities are enough to raise the level of these fluctuations to $O(M)$ values. Thus, we suggest that the level of fluctuations seen in [12] can be attributed to the effect of spatial inhomogeneities in the background plasma pressure and magnetic fields, neglected in NI-MHD.

The four-field model also offers an answer to the fundamental question: Do the effects of plasma compressibility enter the fluctuation dynamics at leading order for $\beta \sim 1$ plasmas, or are the effects of compressibility a higher-order phenomenon enslaved to a leading-order incompressible description, as seen in the NI-MHD model? It is shown that when there are spatial inhomogeneities in the background magnetic field and plasma pressure, the effects of plasma compressibility enter the dynamical equation for the pressure fluctuation at leading order.

Another outstanding question confronting MHD turbulence theory is the nature and scaling of the turbulent energy spectrum. Evidence for anisotropic, probably magnetic field-aligned turbulence is strongly suggested by radio wave scintillation studies of heliospheric and interstellar turbulence. Radio wave scattering in the solar wind close to the Sun is highly anisotropic, with the "long axis" of the irregularities being in the radial, magnetic field-oriented direction and with axial ratios in excess of 10:1 [15,16]. Anisotropic scattering, indicative of anisotropic irregularities, is also a general characteristic of interstellar scattering [17–19]. The observed ratios are smaller than in the heliospheric case, but this may be due to averaging by integration along the line of sight. It seems likely that the axial ratio of the density irregularities exceed the maximum observed factors of 4:1 [18].

The existence of anisotropy in both heliospheric and interstellar plasmas and its implications for spectral scaling laws is a significant challenge for theory. Even when the background consists of a spatially uniform plasma embedded in a constant magnetic field, the precise nature of wave-wave interactions and the form of the energy spectrum has been a subject of some debate [20–25]. All of the studies cited concur, however, that the energy spectrum is strongly anisotropic in the presence of a uniform magnetic field. In the weak-turbulence limit, we present here some new analytical and numerical results on the anisotropic energy spectrum.

The following is a layout of this paper. In Sect. 2, we review the main assumptions and equations underlying the four-field model. In Sect. 3, we derive the NI-MHD model as a special case of the four-field model. In Sect. 4, we present numerical simulation results based on the four-field equations that illustrate the connection between spatial inhomogeneities and enhanced pressure fluctuations. In Sect. 5, we review some exact analytical results on the dominance of three-wave interactions in weak turbulence theory and present the results of a numerical experiment that relies on the analytical results to obtain the anisotropic energy spectrum.

2 The Four-Field Model

The compressible resistive MHD equations are

$$\rho\left(\frac{\partial}{\partial t}+\boldsymbol{v}\cdot\nabla\right)\boldsymbol{v}=-\nabla p+\frac{1}{4\pi}\left(\nabla\times\boldsymbol{B}\right)\times\boldsymbol{B}\,, \tag{1}$$

$$\frac{\partial\boldsymbol{B}}{\partial t}+\nabla\times\left(\boldsymbol{B}\times\boldsymbol{v}+\eta c\boldsymbol{J}\right)=0\,, \tag{2}$$

$$\frac{\partial\rho}{\partial t}+\nabla\cdot\left(\rho\boldsymbol{v}\right)=0\,, \tag{3}$$

$$\frac{d}{dt}\left(\frac{p}{\rho^{\gamma}}\right)=\frac{\gamma-1}{\rho^{\gamma}}\eta\left|\boldsymbol{J}\right|^{2}\,, \tag{4}$$

where ρ is the plasma density, $\boldsymbol{v}$ is the fluid velocity, p is the plasma pressure, $\boldsymbol{B}$ is the magnetic field, $\boldsymbol{J} = c\nabla \times \boldsymbol{B}/4\pi$ is the current density, c is the speed of light, η is the plasma resistivity and γ is the ratio of specific heats. We cast (1)–(4) in dimensionless form by scaling every dependent variable by its characteristic (constant) value, designated by a subscript c (which should be distinguished from the speed of light). We define the sound speed, Alfvén speed, Mach number, Alfvén Mach number, and the plasma beta, respectively, by the relations

$$C_s^2 \equiv (\partial p/\partial \rho)_c \,, \tag{5a}$$
$$V_A^2 \equiv B_c^2/4\pi\rho_c \,, \tag{5b}$$
$$M^2 \equiv v_c^2/C_s^2 \,, \tag{5c}$$
$$M_A^2 \equiv v_c^2/V_A^2 \,, \tag{5d}$$
$$\beta \equiv 4\pi p_c/B_c^2 = M_A^2/\gamma M^2 \,. \tag{5e}$$

In terms of scaled (dimensionless) variables, (1), (2), and (4) can be written

$$\rho\left(\frac{\partial}{\partial t} + \boldsymbol{v}\cdot\nabla\right)\boldsymbol{v} = \frac{1}{\varepsilon^2}\left[-\nabla p + \frac{1}{\beta}(\nabla\times\boldsymbol{B})\times\boldsymbol{B}\right], \tag{6a}$$
$$\frac{\partial \boldsymbol{B}}{\partial t} + \nabla\times(\boldsymbol{B}\times\boldsymbol{v} + \eta\boldsymbol{J}) = 0\,, \tag{6b}$$
$$\frac{d}{dt}\left(\frac{p}{\rho^\gamma}\right) = \frac{\gamma-1}{\beta\rho^\gamma}\eta\,|\boldsymbol{J}|^2 \,, \tag{6c}$$

where $\varepsilon \equiv \sqrt{\gamma}M$, with $\boldsymbol{J} = \nabla\times\boldsymbol{B}$, and (3) retains its present form. (Distance and time are scaled by the system size and the Alfvén time, respectively.) Since (1)–(4) are invariant under Galilean transformations, we choose to work in a reference frame that is stationary with respect to the plasma. The parameter ε, which is essentially the Mach number of the turbulence, is assumed to be much smaller than one and provides the basis for an asymptotic expansion of the dependent variables. We write

$$\begin{aligned}
\boldsymbol{B} &= \boldsymbol{B}_0 + \boldsymbol{B}_1 + \cdots\,, \\
\boldsymbol{v} &= \boldsymbol{v}_1 + \cdots\,, \\
\rho &= \rho_0 + \rho_1 + \cdots\,, \\
p &= p_0 + p_1 + \cdots\,,
\end{aligned} \tag{7}$$

where all $O(1)$ quantities are denoted by subscript zero, and $O(\varepsilon)$ quantities by the subscript one. Note that any large-scale, uniform flow of the plasma with respect to the laboratory frame has been transformed away by moving to the plasma frame (i.e., $\boldsymbol{v}_0 = 0$).

In the four-field model, the background quantities obey the magnetostatic equilibrium condition

$$\nabla p_0 = \frac{1}{\beta}(\nabla\times\boldsymbol{B}_0)\times\boldsymbol{B}_0\,, \tag{8}$$

which continues to hold even as the (first-order) fluctuations evolve in time. In the NI-MHD model, the background quantities are assumed to be

$$p_0 = 1\,, \boldsymbol{B}_0 = \hat{\boldsymbol{z}}\,, \tag{9}$$

which is a special solution of (8). We shall consider the special case (9) in Sect. 3, but propose to develop our model with more general solutions of (8) in mind, allowing for the presence of spatial inhomogeneities in the background plasma variables.

The form of (6a) and (8) motivate the transformations $\boldsymbol{B} \to \sqrt{\beta}\boldsymbol{B}$, $\boldsymbol{J} \to \varepsilon\sqrt{\beta}\boldsymbol{J}$, $\eta \to \eta/\varepsilon^2$, $\boldsymbol{v} \to \boldsymbol{v}/\varepsilon$, $\nabla \to \varepsilon\nabla$, so that $\boldsymbol{B} \sim O(1/\sqrt{\beta})$, $\boldsymbol{v} \sim O(\varepsilon)$, and $\nabla \sim O(1/\varepsilon)$. Under these transformations, (6a) and (8) become

$$\rho\left(\frac{\partial}{\partial t} + \boldsymbol{v}\cdot\nabla\right)\boldsymbol{v} = -\nabla p + (\nabla\times\boldsymbol{B})\times\boldsymbol{B}\,, \tag{10}$$

and

$$\nabla p_0 = (\nabla\times\boldsymbol{B}_0)\times\boldsymbol{B}_0\,, \tag{11}$$

respectively. Also, (3) and (4) may be combined to yield

$$\frac{\partial p}{\partial t} + \boldsymbol{v}\cdot\nabla p + \gamma p\nabla\cdot\boldsymbol{v} = (\gamma-1)\eta\,|\boldsymbol{J}|^2\ . \tag{12}$$

Under these transformations, (6b) remains unchanged while (6c) returns to the form (4), with $\boldsymbol{J} = \nabla\times\boldsymbol{B}$.

As shown by BNS, the momentum equation (10) yields the condition

$$p_1 + \boldsymbol{B}_0\cdot\boldsymbol{B}_1 = 0\,. \tag{13}$$

Hence, the magnetic field fluctuation can be represented as

$$\boldsymbol{B}_1 = \nabla_\perp A\times\boldsymbol{b} - p_1\boldsymbol{b}\,, \tag{14}$$

where $\boldsymbol{b} \equiv \boldsymbol{B}_0/B_0^2$ and A is the perturbed flux function. To $O(1)$, (12) yields the condition

$$\nabla_\perp\cdot\boldsymbol{v}_1 = 0\,, \tag{15}$$

which implies that the perturbed flow is incompressible in the (local) two-dimensional plane perpendicular to $\boldsymbol{B}_0$. By (15), the velocity fluctuation can be represented as

$$\boldsymbol{v}_1 = \nabla_\perp\phi\times\boldsymbol{b} - v_1\boldsymbol{b}\,, \tag{16}$$

where ϕ is a stream function and v_1 is the parallel flow. Equations (14) and (16) contain four field variables: A, p_1, ϕ, and v_1. BNS demonstrate that the compressible resistive MHD equations (1)–(4) can be reduced to the four-field system:

$$\frac{dA}{dt} = \boldsymbol{B}_0 \cdot \nabla\phi + \eta\nabla_\perp^2 A\,, \tag{17}$$

$$\rho_0 \frac{d\Omega}{dt} = DJ + 2\boldsymbol{b} \times \nabla P \cdot \nabla_\perp p_1 - \left(\boldsymbol{b} \cdot \nabla B_0^2\right) J\,, \tag{18}$$

$$\frac{dp_1}{dt} = -\boldsymbol{v}_1 \cdot \nabla p_0 + \frac{\gamma p_0}{\gamma p_0 + B_0^2}\left[2\boldsymbol{v}_1 \cdot \nabla P + Dv_1 + \eta\nabla_\perp^2 p_1\right]\,, \tag{19}$$

$$\rho_0 \frac{dv_1}{dt} = Dp_1 + \boldsymbol{B}_1 \cdot \nabla p_0\,, \tag{20}$$

Here

$$\Omega \equiv -\nabla_\perp^2 \phi\,, \tag{21a}$$

$$J \equiv -\nabla_\perp^2 A\,, \tag{21b}$$

$$P \equiv p_0 + B_0^2/2\,, \tag{21c}$$

$$\frac{d}{dt} \equiv \frac{\partial}{\partial t} + \boldsymbol{v} \cdot \nabla_\perp\,, \tag{21d}$$

$$D \equiv (\boldsymbol{B}_0 + \boldsymbol{B}_{1\perp}) \cdot \nabla\,, \tag{21e}$$

$$\nabla_\perp \equiv \nabla - \hat{\boldsymbol{B}}_0\hat{\boldsymbol{B}}_0 \cdot \nabla\,,\;\; \hat{\boldsymbol{B}}_0 \equiv \boldsymbol{B}_0/B_0\,, \tag{21f}$$

$$\rho_0 \equiv p_0^{1/\gamma}\,. \tag{21g}$$

The derivation of the four-field equations by BNS does not restrict the background inhomogeneous magnetic field and pressure in any way except for the requirement that they satisfy (8) which permits an infinity of solutions with spatial dependencies in the magnetic field as well as the pressure. For very low or zero values of β, (8) permits spatially dependent force-free magnetic fields of which the vacuum field is a special case. The solution (9) which is the starting point of NI-MHD is, in fact, the simplest non-trivial example of a vacuum field. In Sect. 3, we derive the equations for the NI-MHD model as a special case of the four-field equations.

3 The NI-MHD Model

In order to derive the NI-MHD equations from the more general four-field equations, it is convenient to write

$$\boldsymbol{B}_0 = \frac{\hat{\boldsymbol{z}}}{\sqrt{\beta}} + \boldsymbol{B}_s\,, \tag{22}$$

where $\boldsymbol{B}_s$ represents the spatially inhomogeneous part of the background magnetic field which has been separated from a constant part. The separation assumed in writing (22) is not required for the validity of the four-field equations, but allows us to establish the conditions under which the NI-MHD

equations hold. We now observe:
(i) If $\boldsymbol{B}_s \to 0$, then (17) and (18) simplify to the NI-MHD system with two field variables A and ϕ. Equations (19) and (20) decouple from (17) and (18) in this limit, and we recover the results of ZM. The equations for A and ϕ in the NI-MHD model are

$$\frac{dA}{dt} = \boldsymbol{B}_0 \cdot \nabla\phi + \eta\nabla_\perp^2 A\,, \tag{23}$$

$$\rho_0 \frac{d\Omega}{dt} = DJ\,. \tag{24}$$

(ii) The case $\beta \ll 1$ is effectively the same as $\boldsymbol{B}_s \to 0$, and conclusion (i) again holds.

In general, if $\beta \sim 1$, the effect of compressibility enters the dynamics at leading order and cannot be enslaved to an incompressible flow field. In this general case, $p_1 \neq 0$ and $\rho_1 \neq 0$ which differs from the predictions of the NI-MHD model. Due to the dynamical coupling at leading order between the pressure fluctuations and the flow field, brought about by the presence of spatial inhomogeneities, the first-order pressure and density fluctuations, even if they are small initially, can increase to the level of the Mach number.

Before we conclude this section, we remark on the role of a pressure-balanced structure (PBS) in the four-field model. An interesting simplification of the four-field equations occurs if we specialize to a PBS which obeys the relation $P \equiv p_0 + B_0^2/2 =$ constant. Then (17) and (18) decouple from (19) and (20), but (18) contains the additional term $\left(\boldsymbol{b} \cdot \nabla B_0^2\right) J$, absent in NI-MHD. This implies that pressure-balanced structures obey dynamical equations slightly more general than NI-MHD. However, we repeat for emphasis that the equation governing pressure fluctuations associated with a PBS in the four-field model remains decoupled from (18) and (19) (as in NI-MHD). This suggests that the mere presence of spatial inhomogeneities in a PBS is not enough to raise the level of pressure (or density) fluctuations to order M if they are small initially. In other words, if we are to understand the data on pressure fluctuations presented in Fig. 3 of [12] within the framework of the four-field model, we cannot do so by merely generalizing (8) to include only pressure-balanced structures. The background magnetic field must also include inhomogeneities associated with the curvature of magnetic field lines, absent in a PBS. The initial condition discussed in Sect. 4 does not obey the condition $P \equiv p_0 + B_0^2/2 =$ constant which, as we show below, leads to the generation of density fluctuations of order M.

4 Four-Field Simulations: Implications for Pressure Fluctuations

We represent the initial magnetic field as

$$\boldsymbol{B}_0 = \nabla_{\perp 0} A_0(x, y) \times \hat{\boldsymbol{z}} + B_0 \hat{\boldsymbol{z}}\,, \tag{25}$$

where

$$\nabla_{\perp 0} = \hat{\boldsymbol{x}} \frac{\partial}{\partial x} + \hat{\boldsymbol{y}} \frac{\partial}{\partial y} , \tag{26}$$

and $A_0(x, y)$ is the mean flux representing the spatially inhomogeneous component of the initial magnetic field in the x-y plane. Assuming periodic boundary conditions in x and y, an exact solution of (11) is

$$A_0 = a \left(\cos 2\pi x - \sin 2\pi y \right) , \tag{27}$$

with

$$p_0 = 1 + 2\pi^2 A_0^2 . \tag{28}$$

In the initial state, we take the plasma β to be equal to one, held fixed at this value in all the four-field runs. Since the four-field equations have been derived with the ordering $p_0 \leq O(1)$, and p_0 is assumed to have the functional form (28), we must constrain the function A_0 by the inequality $2\pi^2 A_0^2 \leq 1$. Since the maximum magnitude of A_0 is $2a$, the parameter a is constrained by the inequality $a < 0.1125$.

In order to follow the time-evolution of this initial state, we have developed a 2 1/2-D pseudo-spectral code for the four-field equations. Periodic boundary conditions are applied in x and y, and all dependent field variables are represented in Fourier series, such as

$$\phi(x, y) = \sum_{mn} \phi_{mn} e^{2\pi i (mx + ny)} , \tag{29}$$

where m and n are integers. We refer the reader to BNS for more details of the numerical method, and limit ourselves here to a discussion of the link between spatial inhomogeneities and enhanced pressure fluctuations.

Figure 1 shows a contour plot of level surfaces of the mean flux A_0 on the x-y plane. This is a 2D projection of four flux tubes carrying currents, two parallel and two anti-parallel to $\hat{\boldsymbol{z}}$. The tubes are unstable to the coalescence instability which arises from the tendency of two opposite current-carrying tubes to attract each other. The tubes coalesce, squeezing magnetic flux and generating thin current sheets in-between them. Due to the presence of finite resistivity, magnetic reconnection occurs at the separatrices, facilitating the process of coalescence.

The results of NI-MHD are recovered as a smooth limit of four-field MHD when the limit $a \to 0$ is taken. When a is very small ($\leq 10^{-6}$), numerical results demonstrate that the overall dynamics of the four-field system is very similar to NI-MHD dynamics ($a = 0$). However, even with moderate values a ($= 10^{-4}$, 10^{-3}), there are significant dynamical differences between four-field and NI-MHD dynamics.

Figure 2 shows the level of p_{rms} in the quasi-saturated state (indicated by diamonds) as a function of M for different values of a, with $M(t = 0) \approx 0.01$. In order to quantify the approximate saturation level of the fluctuations, two

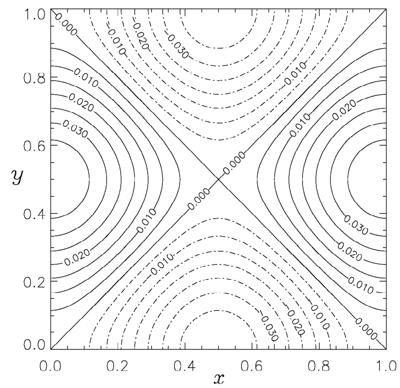

Fig. 1. Contour plot of the background inhomogeneous field A_0 [given by (25)]

lines are drawn: a solid line corresponding to the level $p_{\rm rms} = M$, and a dashed line corresponding to the level $p_{\rm rms} = M^2$. We note that saturated values of $p_{\rm rms}$ approach the line $p_{\rm rms} = M$ as the parameter a increases. Even for values of a as small as 0.04, the condition $p_{\rm rms} = M$ is attained. This trend persists for higher values of a. Similar qualitative features also appear for higher initial values of M, as shown by data from runs with $M(t = 0) \approx$ 0.1 (indicated by stars).

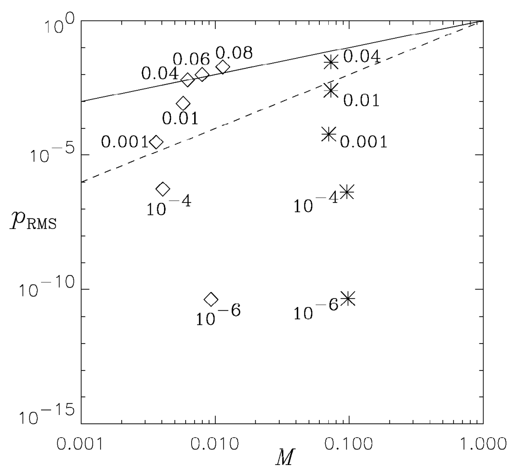

Fig. 2. The level of the root-mean-square value of the first order pressure $p_{\rm rms}$ in the quasi-saturated state as a function of the Mach number M for different values of a, for $M(t = 0) \approx 0.01$ (diamonds) and $M(t = 0) \approx 0.1$ (stars). The solid line corresponds to $p_{\rm rms} = M$, and the dashed line to $p_{\rm rms} = M^2$

Note that when a is small enough ($\leq 10^{-4}$) the quasi-saturated level of the pressure fluctuation lies below the $p_{\rm rms} = M^2$ line. This implies that the contribution from p_1 to the total pressure fluctuation may actually become subdominant to the second order contribution p_2 which is not zero in general. In the small a limit, we thus recover ZM's result that the pressure fluctuations are second order.

We have focused above on the issue of the scaling of the pressure fluctuations with the Mach number of the turbulence, identified in [12] as an outstanding feature of observations. The numerical results show that in the presence of spatial inhomogeneities, the four-field model produces density fluctuations that increase from $O(M^2)$ to $O(M)$ as the inhomogeneity parameter is increased. We thus conclude that if heliospheric and interstellar turbulence exists in a plasma with large-scale, non-turbulent spatial gradients, one expects the pressure fluctuations to be of significantly larger magnitude than suggested in nearly incompressible models such as pseudosound.

5 Anisotropic Spectra in Weak Turbulence Theory

In the presence of a directed magnetic field, MHD turbulence tends to exhibit a pronounced anisotropy. The main goal of this section is to examine, in the limit of weak turbulence, the nature and scaling of the anisotropic spectrum in a plasma permeated by a spatially uniform magnetic field $\boldsymbol{B} = B_0\hat{\boldsymbol{z}}$. As discussed above, the four-field equations reduce in this simple case to the NI-MHD (or RMHD) equations.

Weak magnetohydrodynamic turbulence in the presence of a uniform magnetic field is dominated by three-wave interactions that mediate the collisions of shear-Alfvén wave packets propagating in opposite directions parallel to the magnetic field. This dominance of three-wave interactions has been known since the advent of the Iroshnikov–Kraichnan theory [26,27], and has been the subject of a few recent papers [21,22,25]. Using the ideal NI-MHD equations, Ng and Bhattacharjee (NB) [22] calculate in closed form the three-wave and four-wave interaction terms, and show the former to be asymptotically dominant if the wave packets have non-zero $k_\parallel = 0$ components. To keep this discussion self-contained, we begin with a summary of relevant results by NB.

The ideal NI-MHD equations (23) and (24) can be rewritten as the system of equations,

$$\begin{aligned} \frac{\partial \Omega}{\partial t} - \frac{\partial J}{\partial z} &= [A, J] - [\phi, \Omega]\,, \\ \frac{\partial A}{\partial t} - \frac{\partial \phi}{\partial z} &= -[\phi, A]\,, \end{aligned} \tag{30}$$

where the magnetic field is given by $\boldsymbol{B} = \hat{\boldsymbol{z}} + \nabla_\perp A \times \hat{\boldsymbol{z}}$ with A as the magnetic flux function, the flow velocity is given by $\boldsymbol{v} = \nabla_\perp \phi \times \hat{\boldsymbol{z}}$ with ϕ as the stream function, and $[\phi, A] \equiv \phi_y A_x - \phi_x A_y$. The parallel vorticity is then $\Omega = -\nabla_\perp^2 \phi$, and the parallel current density is $J = -\nabla_\perp^2 A$. Note that we have normalized the background uniform magnetic field in the $\hat{\boldsymbol{z}}$-direction to have unit magnitude, and the density has been chosen so that the Alfvén speed $V_A = 1$.

For weak interactions between two colliding shear-Alfvén wave packets $f^\pm$ traveling in the $\pm\hat{\boldsymbol{z}}$ directions, we write perturbative solutions of the form

$$\begin{aligned} \phi &= f^-(\boldsymbol{x}_\perp, z^-) + f^+(\boldsymbol{x}_\perp, z^+) + \phi_1 + \phi_2 + \cdots\,, \\ A &= f^-(\boldsymbol{x}_\perp, z^-) - f^+(\boldsymbol{x}_\perp, z^+) + A_1 + A_2 + \cdots\,, \end{aligned} \tag{31}$$

where $\boldsymbol{x}_\perp = (x, y)$ is perpendicular to $\hat{\boldsymbol{z}}$ and $z^\pm = z \mp t$. Here $f^\pm(\boldsymbol{x}_\perp, z^\pm)$ represents Alfvén wave packets that propagate non-dispersively with the Alfvén speed $V_A = 1$. These exact solutions propagate inward from $z = \mp\infty$ at $t \to -\infty$, retaining their form, until they collide. Because of the intrinsic nonlinearity of (30), the interaction of two colliding wave packets cannot be simply described by linear combinations of $f^\pm(\boldsymbol{x}_\perp, z^\pm)$, for the linear combinations are not exact solutions of (30). For given zero-order fields $f^\pm$, we can then calculate the first-order fields in (31) from the equations

$$\frac{\partial \Omega_1}{\partial t} - \frac{\partial J_1}{\partial z} = 2\left\{\left[f^+, \nabla_\perp^2 f^-\right] + \left[f^-, \nabla_\perp^2 f^+\right]\right\} \equiv F\,, \tag{32a}$$

$$\frac{\partial A_1}{\partial t} - \frac{\partial \phi_1}{\partial z} = 2[f^-, f^+] \equiv G\,. \tag{32b}$$

This is a radiation equation for the first-order fields, with the source term determined by the overlap of the given zero-order fields f^+ and f^-. The source term is localized both in space and in time, assuming that the functional forms of $f^\pm$ are chosen so that the wave packets are localized in z. The asymptotic expression of ϕ_1, A_1 can be written,

$$\phi_1(\boldsymbol{x}_\perp, t \to \infty) \to f_1^-(\boldsymbol{x}_\perp, z^-) + f_1^+(\boldsymbol{x}_\perp, z^+)\,, \tag{33a}$$

$$A_1(\boldsymbol{x}_\perp, t \to \infty) \to f_1^-(\boldsymbol{x}_\perp, z^-) - f_1^+(\boldsymbol{x}_\perp, z^+)\,, \tag{33b}$$

where

$$f_1^\pm(\boldsymbol{x}_\perp, z) = \pi \int \left[\tilde{F}'(\boldsymbol{k}, \pm k_z) \mp \tilde{G}(\boldsymbol{k}, \pm k_z)\right] e^{i\boldsymbol{k}\cdot\boldsymbol{x}} d\boldsymbol{k}\,, \tag{34}$$

with $\tilde{F}'(\boldsymbol{k}, \omega) \equiv \tilde{F}(\boldsymbol{k}, \omega)/k_\perp^2$ and $\tilde{F}(\boldsymbol{k}, \omega)$ is the Fourier transform of $F(\boldsymbol{x}, t)$, defined by

$$F(\boldsymbol{x}, t) = \int \tilde{F}(\boldsymbol{k}, \omega) e^{i(\boldsymbol{k}\cdot\boldsymbol{x} - \omega t)} d\boldsymbol{k} d\omega\,.$$

The Fourier transform $\tilde{G}(\boldsymbol{k}, \omega)$ is similarly defined.

To simplify the calculation that follows, we consider the case in which the functions $f^\pm(\boldsymbol{x}_\perp, z)$ are separable, i.e., $f^\pm(\boldsymbol{x}_\perp, z) = f_\perp^\pm(\boldsymbol{x}_\perp) f^\pm(z)$. (The calculation can also be carried through in the more general case when $f^\pm(\boldsymbol{x}_\perp, z)$

can be written as a sum of such separable terms, which is always possible as long as the boundary conditions in $\boldsymbol{x}_\perp$ are periodic.) Then we can write

$$F(\boldsymbol{x},t) = F_\perp(\boldsymbol{x}_\perp)f^+(z^+)f^-(z^-)\,, G(\boldsymbol{x},t) = G_\perp(\boldsymbol{x}_\perp)f^+(z^+)f^-(z^-)\,,$$
$$\tilde{F}(\boldsymbol{k},\omega) = \frac{1}{2}\tilde{F}_\perp(\boldsymbol{k}_\perp)\tilde{f}^+(\kappa^+)\tilde{f}^-(\kappa^-)\,, \tilde{G}(\boldsymbol{k},\omega) = \frac{1}{2}\tilde{G}_\perp(\boldsymbol{k}_\perp)\tilde{f}^+(\kappa^+)\tilde{f}^-(\kappa^-)\,,$$

where $\kappa^\pm \equiv (k_z \pm \omega)/2$, $\tilde{f}(\kappa^\pm)$ is the one dimensional Fourier transforms of $f^\pm(z^\pm)$, $\tilde{F}_\perp$ and $\tilde{G}_\perp$ are the two dimensional Fourier transforms of $F_\perp$ and $G_\perp$. We obtain

$$f_1^\pm(\boldsymbol{x}_\perp, z^\pm) = \pi u_\perp^\pm(\boldsymbol{x}_\perp)\tilde{f}^\mp(0)f^\pm(z^\pm)/2\,, \tag{35}$$

where

$$u_\perp^\pm(\boldsymbol{x}_\perp) = \int \left[\tilde{F}'_\perp \mp \tilde{G}_\perp\right] e^{i\boldsymbol{k}_\perp\cdot\boldsymbol{x}_\perp} d\boldsymbol{k}_\perp\,, \tag{36}$$

and $\tilde{f}^\mp(0)$ is the $k_z = 0$ Fourier component of $f^\pm(z)$, with $\tilde{F}'_\perp(\boldsymbol{k}_\perp) \equiv \tilde{F}_\perp(\boldsymbol{k}_\perp)/k_\perp^2$.

We note that the expression (36) for three-wave interactions preserves the z-dependence of the zero-order fields. This implies that there is no energy transfer parallel to the magnetic field. However, as pointed out by NB, four-wave interactions do not generally preserve the z–dependence of the zero-order fields and exhibit harmonic generation, and can, in principle, contribute to parallel energy transfer. Since three-wave couplings are much larger than four-wave couplings for weak turbulence, we neglect the effect of parallel energy transfer. Using (36), we can then calculate explicitly the scaling of three-wave interactions. Specifically, our objective is to calculate the spectral indices of the three-wave fields as functions of the spectral indices of the zero-order fields.

Imposing periodic boundary condition in $\boldsymbol{x}_\perp$, we can write

$$f_\perp^\pm(\boldsymbol{x}_\perp) = \sum_{mn} f_{mn}^\pm e^{2\pi i(mx+ny)}\,, \tag{37}$$

where $f_{mn}^\pm$ are constants. Let the energy spectra have the form

$$E_\pm(k_\perp) \propto k_\perp^{-\mu_\pm} \;\text{ or }\; \left|f_{mn}^\pm\right| \propto (m^2+n^2)^{-(3+\mu_\pm)/4}\,, \tag{38}$$

where $\mu_\pm$ are the spectral indices. The profiles of the three-wave interaction fields can then be calculated by

$$u_\perp^\pm(\boldsymbol{x}_\perp) = \sum_{mn}\left[F'_{mn} \mp G_{mn}\right] e^{2\pi i(mx+ny)} = \sum_{mn} u_{mn}^\pm e^{2\pi i(mx+ny)}\,, \tag{39}$$

having spectral indices $\nu_\pm$, i.e., $|u_{mn}^\pm| \propto (m^2+n^2)^{-(3+\nu_\pm)/4}$, where $F'_{mn} = F_{mn}/(2\pi)^2(m^2+n^2)$ with

$$\sum_{mn} F_{mn}e^{2\pi i(mx+ny)} = 2\left\{\left[f_\perp^+, \nabla_\perp^2 f_\perp^-\right] + \left[f_\perp^-, \nabla_\perp^2 f_\perp^+\right]\right\}\,,$$
$$\sum_{mn} G_{mn}e^{2\pi i(mx+ny)} = 2[f_\perp^-, f_\perp^+]\,. \tag{40}$$

It is found both analytically and numerically that [28]

$$\nu_+ \approx \mu_- \,, \quad \nu_- \approx \mu_- - 2 \quad \text{for} \quad \mu_+ \gg \mu_- \,, \tag{41a}$$

$$\nu_+ \approx \mu_+ - 2 \,, \quad \nu_- \approx \mu_+ \quad \text{for} \quad \mu_+ \ll \mu_- \,. \tag{41b}$$

Our main objective now is to determine how the spectrum of an Alfvén wave packet changes in time after many collisions with wave packets coming from the opposite direction. To be specific, let us consider the evolution of a f^+ field interacting with a sequence of random f^- fields. From (39) and (40), we deduce that

$$\frac{\partial \Psi^+}{\partial t} = -[f^-, \Psi^+] + [f_x^-, f_x^+] + [f_y^-, f_y^+] \,, \tag{42}$$

where $\Psi^+ = -\nabla_\perp^2 f^+$. Numerically, the Fourier amplitudes f_{mn}^- are randomly chosen for a given spectral index μ_- in every time step τ_A. The time step has to be chosen small enough to satisfy the weak turbulence assumption and to represent the fact that each wave packet in the sequence of f^- is uncorrelated with each other. Also, in order to have a better resolved inertial range of the f^+ spectrum, a hyper-dissipation term of the form $\eta \nabla_\perp^6 \Psi^+$ is added to the right hand side of (42) with a suitably chosen η so that the inertial range is resolved with an index that is insensitive to the value of η. Equation (42) is then solved by a pseudo-spectral method for different values of μ_- and for different levels of resolution, up to 1024^2, until the f^+ spectrum reaches a quasi-steady state when inertial range index is roughly a constant with only small temporal fluctuations.

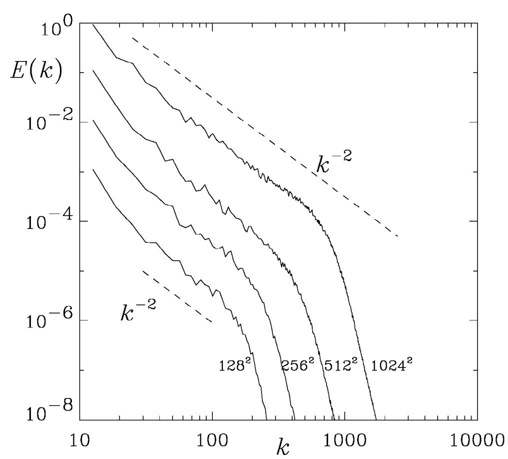

Fig. 3. The spectra of the f^+ field with $\mu_- = 2$ for different resolution level indication beside each curve. A vertical separation is added in between each pair of spectra for clarity

Figure 3 shows the f^+ spectra for the case with $\mu_- = 2$ for different resolution levels. We see that the inertial range for all runs roughly have the same index, $\mu_+ \approx 2$. In this case, we obtain the anisotropic energy spectrum $k_\perp^{-2}$. This result has been derived earlier by dimensional analysis [20,22,24] and more recently, by careful analytical and numerical work based on a weak turbulence formalism [25].

Acknowledgments

This research is supported by the National Science Foundation Grant No. ATM-9801709.

References

1. Zank, G. P., Matthaeus, W. H. (1992) The equations of reduced magnetohydrodynamics. J. Plasma Phys. **48**, 85
2. Zank, G. P., Matthaeus, W. H. (1993) Nearly incompressible fluids. II: Magnetohydrodynamics, turbulence, and waves. Phys. Fluids A **5**, 257
3. Lighthill, M. J. (1952) On sound generated aerodynamically, I. General Theory. Proc. R. Soc. London Ser. A **211**, 564
4. Montgomery, D., Brown, M., Matthaeus, W. H. (1987) Density fluctuation spectra in magnetohydrodynamic turbulence. J. Geophys. Res. **92**, 282
5. Shebalin, J. V., Montgomery, D. (1988) Turbulent magnetohydrodynamic density fluctuations. J. Plasma Phys. **39**, 339
6. Matthaeus, W., Brown, M. R. (1988) Nearly incompressible magnetohydrodynamics at low Mach-number. Phys. Fluids **31**, 3634
7. Zank, G. P., Matthaeus, W. H. (1991) The equations of nearly incompressible fluids. I. Hydrodynamics, turbulence and waves. Phys. Fluids A **3**, 69
8. Grappin, Velli, R. M., Mangeney, A. (1991) “Alfvénic” versus “standard” turbulence in the solar wind. Ann. Geophys. **9**, 416
9. Kliatskin, V. I. (1966) Homogeneous isotropic turbulence in weakly compressible media. Izv. Atmos. Oceanic Phys. **2**, 474
10. Strauss, H. R. (1976) Nonlinear three-dimensional magnetohydrodynamics of noncircular tokamaks. Phys. Fluids **19**, 134
11. Matthaeus, W. H., Klein, L. W., Ghosh, S., Brown, M. R. (1991) Nearly incompressible magnetohydrodynamics and solar wind fluctuations. J. Geophys. Res. **96**, 5421
12. Tu, C.-Y., Marsch, E. (1994) On the nature of compressive fluctuations in the solar wind. J. Geophys. Res. **99**, 21481
13. Bavassano, B., Bruno, R., Klein, L. (1995) Density-temperature correlation in Solar-wind magnetohydrodynamic fluctuations — a test for nearly incompressible models. J. Geophys. Res. **100**, 5871
14. Bhattacharjee, A., Ng, C. S., Spangler, S. R. (1998) Weakly compressible magnetohydrodynamic turbulence in the solar wind and the interstellar medium. Astrophys. J. **494**, 409
15. Armstrong, J. W., Coles, W. A., Kojima, K., Rickett, B. J. (1990) Observations of field-aligned density fluctuations in the inner solar wind. Astrophys. J. **358**, 685

16. Grall, R. R., Coles, W. A., Spangler, S. R., Sakurai, T., Harmon, J. K. (1997) Observations of field-aligned density microstructure near the Sun. J. Geophys. Res. **102**, 263
17. Wilkinson, P. N., Narayan, R., Spencer, R. E. (1994) MNRAS **269**, 67
18. Frail, D. A., Diamond, P. J., Cordes, J. M., Van Langevelde, H. J. (1994) Anisotropic scattering of OH/IR stars toward the galactic center. Astrophys. J. **427**, L43
19. Molnar, L. A., Mutel, R. L., Reid, M. J., Johnston, K. J. (1995) Interstellar scattering toward cygnus X-3: measurements of anisotropy and of the inner scale. Astrophys. J. **438**, 708
20. Sridhar, S., Goldreich, P. (1994) Toward a theory of interstellar turbulence. I. weak Alfvénic turbulence. Astrophys. J. **432**, 612
21. Montgomery, D., Matthaeus, W. H. (1995) Anisotropic modal energy transfer in interstellar turbulence. Astrophys. J. **447**, 706
22. Ng, C. S., Bhattacharjee, A. (1996) Interaction of shear-Alfvén wave packets: implication for weak magnetohydrodynamic turbulence in astrophysical plasmas. Astrophys. J. **465**, 845
23. Chen, S, Kraichnan, R. H. (1997) Inhibition of turbulence cascade by sweep. J. Plasma Phys. **57**, 187
24. Goldreich, P., Sridhar, S. (1997) Magnetohydrodynamic turbulence revisited. Astrophys. J. **485**, 680
25. Galtier, S., Nazarenko, S., Newell, A. C., Pouquet, A. (1998) A weak turbulence theory for incompressible magnetohydrodynamics. These proceedings
26. Iroshnikov, P. S. (1963) The turbulence of a conducting fluid in a strong magnetic field. Astron. Zh. **40**, 742
27. Kraichnan, R. H. (1965) Inertial-range spectrum of hydromagnetic turbulence. Phys. Fluids **8** 1385
28. Ng, C. S., Bhattacharjee, A. (1997) Scaling of anisotropic spectra due to the weak interaction of shear-Alfvén wave packets. Phys. Plasma **4**, 605